Synthesis of Triblock Copolymer Brushes by Surface-Initiated Atom Transfer Radical Polymerization

Jong-Bum Kim, Wenxi Huang, Merlin L. Bruening,* and Gregory L. Baker*

Department of Chemistry and Center for Sensor Materials, Michigan State University, East Lansing, Michigan 48824

Received October 3, 2001; Revised Manuscript Received April 16, 2002

ABSTRACT: Surface-tethered triblock copolymers composed of poly(methyl acrylate), poly(methyl methacrylate), and poly(2-hydroxyethyl methacrylate) were grown from gold substrates by a series of atom transfer radical polymerizations at ambient temperature. GPC determinations of the molecular weights of desorbed triblock homopolymers suggest that this method can yield relatively homogeneous polymer brushes. To quench polymerization after the synthesis of each block, films were either exposed to a large excess of $Cu(II)Br_2$ or simply rinsed with solvent. Comparison of the thicknesses of multiblock homopolymer films with the thicknesses of films prepared using a single initiation step shows that in the Cu(II) quenching approach >95% of the active chains support growth of an additional block. However, for simple solvent rinsing between blocks, only 85−90% of active chains were preserved during the quenching step.

Introduction

Block copolymers are attractive materials because of their ability to phase separate and self-assemble into spherical, rodlike, and lamellar geometries. When deposited on surfaces, the orientation of the phase-segregated structure can be controlled by selective adsorption of one block[1] or by the application of external fields.[2] These phenomena lead to formation of patterns that can be used as templates for further materials deposition. Recent examples of materials patterned in this way include vertically oriented nanowires[3] and SiO_2 posts.[4]

Tethering multiblock copolymers to surfaces is particularly interesting because it provides responsive, controllable interfaces[5] with nanoscale features.[6] Brittain et al. showed that copolymer brushes reversibly self-organize on exposure to different solvents.[7−9] The topology of multiblock copolymer brushes also suggests their use in forming multilayered materials where the layers can be arranged in a predetermined order. Growth of such films from tethered initiators complements other layer-by-layer schemes for thin film deposition.[10]

The most common approaches for synthesizing surface-tethered block copolymers are (1) the preparation of immobilized polymeric macroinitiators that can be used later to initiate the polymerization of a second block and (2) the sequential addition of two or more monomers during polymerization from a surface. The first strategy often employs different polymerization mechanisms to form each block, while the second method is restricted to monomers that can be polymerized sequentially. Examples of the macroinitiator approach for preparation of surface-tethered copolymers include the synthesis of polystyrene-*b*-poly(methyl methacrylate) (PS-*b*-PMMA), polystyrene-*b*-poly(methyl acrylate) (PS-*b*-PMA), and PS-*b*-poly(*N*,*N*-(dimethylamino)ethyl methacrylate) by sequential carbocationic polymerization and atom transfer radical polymerization (ATRP).[7,11] PS-*b*-PMMA was also prepared from surface-immobilized azo initiators by successive reverse-ATRP and ATRP.[8] Using the second approach, surface-tethered PS-*b*-PMA and PS-*b*-poly(*tert*-butyl acrylate) were synthesized by sequential ATRP,[12] and surface-immobilized alkoxyamines were used for the preparation of PS-*b*-poly(styrene-*co*-methyl methacrylate) brushes.[13]

This study extends the surface-initiated synthesis of block copolymers from diblock to triblock systems using low-temperature ATRP. Specifically, we synthesized PMMA-*b*-PMA-*b*-poly(hydroxyethyl methacrylate) (PHEMA) because synthesis of each block can be followed by FTIR spectroscopy and because PHEMA may introduce phase segregation to this system. The major focus of this work is determining the efficiency with which additional blocks can be added to chains growing from a surface. When working with polymers composed of many blocks, this efficiency becomes especially important as shown by significant thickness differences between heptablock films prepared using two different strategies for radical quenching between the deposition of blocks.

ATRP is very attractive for formation of block copolymers because radical generation is in principle "reversible" due to an equilibrium between the active (radical/$Cu(II)Br_2$/ligand) and dormant (initiator/Cu(I)Br/ligand) states. Scheme 1 shows the reversible generation and quenching of a radical in the ATRP of methyl methacrylate (MMA). Ignoring chain transfer reactions, polymer radical **I** can either undergo further polymerization by adding more monomer, convert to the dormant macroinitiator **II**, or terminate through bimolecular coupling or disproportionation reactions. Since the radical concentration in ATRP is usually low,[14] termination is the least common scenario. We can intentionally favor the formation of the dormant macroinitiator by adding a high concentration of $Cu(II)Br_2$ to capture the radicals and shift the equilibrium to the dormant state.[8] This quenching should effectively stop polymerization and keep growing chain ends alive for polymerization of subsequent blocks.

* To whom correspondence should be addressed. Phone (517) 355-9715, ext. 160 or 237; Fax (517) 353-1793; e-mail bakerg@msu.edu, bruening@cem.msu.edu.

10.1021/ma011736z CCC: $22.00
Published on Web 06/04/2002

Scheme 1

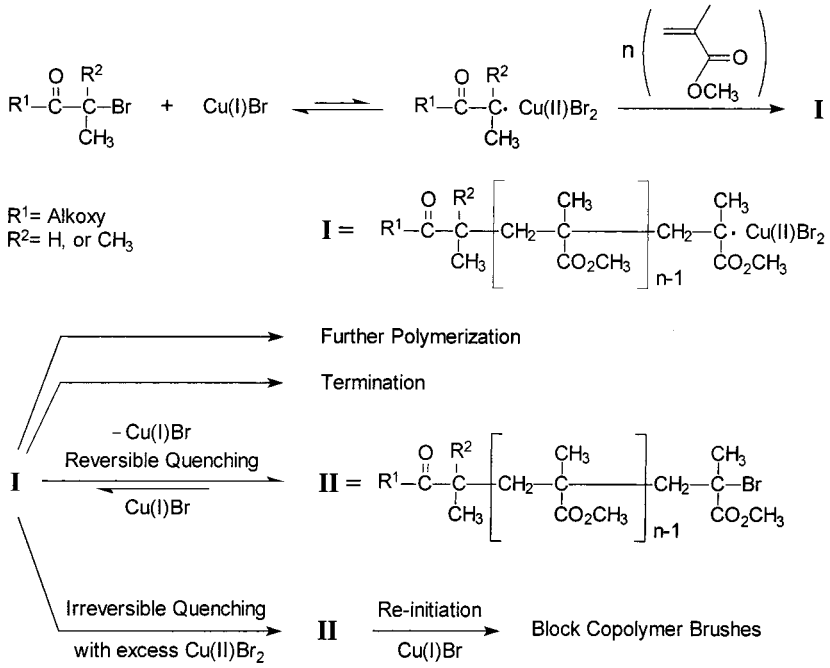

This quenching and reinitiation (QR) approach is particularly powerful for the preparation of surface-tethered block copolymers because the polymeric radical is confined to the surface, and the quenching step simply involves transferring substrates to a concentrated Cu(II)Br_2 solution that does not contain Cu(I)Br. Thus, the length of the polymer chain is controlled by the elapsed polymerization time before exposure to the Cu(II)Br_2 solution. After rinsing to remove residual Cu(II)Br_2, the polymerization can be reinitiated to extend the chains, or multiblock copolymers can be synthesized by simply switching to a different monomer after each cycle. The main advantages of this approach are the facile synthetic procedure, easy control over the thickness of each polymeric layer, restriction of polymerization to surface-bound chains, and a low polymerization temperature that is compatible with temperature-sensitive substrates. Additionally, because no detectable polymerization occurs in solution, exhaustive extraction is not needed for cleaning films between deposition of different blocks.[13]

Experimental Section

Materials. THF (Aldrich, 99%) was purified by distillation from calcium hydride followed by distillation from sodium/benzophenone ketyl. Acetonitrile (Merck, HPLC grade) was passed through an activated basic alumina column and fractionally distilled over calcium hydride. Triethylamine (Aldrich, 99.5%) was distilled from calcium hydride under an argon atmosphere at reduced pressure. Methyl acrylate (MA) (Aldrich, 99%) and methyl methacrylate (MMA) (Aldrich, 99%) were distilled from powdered KOH under ambient pressure. 2-Hydroxyethyl methacrylate (HEMA) (Aldrich, 97%) was passed through two basic alumina columns to remove inhibitor. After purification, all solvents and monomers were degassed using three freeze−pump−thaw cycles and then transferred into a drybox. Tris[2-(dimethylamino)ethyl]amine[15] (Me_6-TREN) and 4,4′-di-*n*-nonyl-2,2′-bipyridine[16] (dnNbpy) were prepared by literature procedures. 11-Mercapto-1-undecanol (MUD) (Aldrich, 97%), 2-bromopropionyl bromide (Aldrich, 97%), Cu(I)Br (Aldrich, 99.999%), and Cu(II)Br_2 (Aldrich, 99.999%) were used as received.

Preparation of Initiator-Immobilized Substrate, 1. Gold-coated Si wafers (200 nm of gold sputtered on 20 nm of Cr on Si(100) wafers) were cleaned in a UV/O_3 chamber for 15 min, immersed in deionized water for 15 min, and dried under a flow of N_2 just before use. A self-assembled monolayer (SAM) of MUD was obtained by immersing the gold-coated Si substrate in a 1 mM MUD solution for 1 day, and the MUD SAM was washed with copious amounts of ethanol and deionized water and dried under N_2. The ellipsometric thickness of the MUD layer was 12 ± 1 Å. To produce the initiator-anchored surface, **1** (Scheme 2), the MUD SAM was immersed for ∼10 s in 5 mL of 0.12 M triethylamine in dry THF at ∼0 °C, after which 5 mL of 0.1 M 2-bromopropionyl bromide (2-BPB) in dry THF was added dropwise while gently agitating the triethylamine solution. During the addition of 2-BPB, we tilted the reaction vial at different angles to ensure that the reaction surface was well exposed to the incoming 2-BPB solution. This initiator-immobilization reaction was performed in a helium-filled drybox. Upon addition of 2-BPB, a white precipitate formed immediately, which presumably was triethylamine hydrobromide. After the reaction (∼3 min), the surface was washed with fresh THF several times and allowed to dry. Once the substrate was taken out of the drybox, it was rinsed sequentially with EtOAc, EtOH, and deionized water and dried under N_2. Initiator immobilization was apparent from the appearance of a carbonyl peak at 1743 cm^{-1} in the reflectance FTIR spectrum of this film.[17]

Polymerization Procedures. Preparation of monomer/catalyst solutions, polymerizations, and QR procedures were done in a drybox filled with helium. Three kinds of monomer (MA, MMA, and HEMA) solutions were prepared in 1:1 (v/v) CH_3CN:THF. Each solution contained monomer (2 M), Cu(I)Br/Me_6TREN (2 mM), and Cu(II)Br_2/2(dnNbpy) (0.6 mM). Each block of the polymer brush was synthesized by dipping substrates **1**, **2**, or **3** (Scheme 2) in the appropriate monomer solution and then quenching as described below. Polymerizations were run at 25 °C for the first and second blocks (PMA and PMMA) and at 40 °C for the third block (PHEMA), and the reaction times for formation of each block were 20 min, 40 min, and 5 h, respectively. After polymerization, the substrate was removed from the solution and sequentially immersed in three vials of CH_3CN-THF (1:1) and three vials of THF. This procedure avoids drying of the film and consequent deposition of solids that are difficult to remove from the substrate surface. For model studies of heptablock synthesis, the polymerizations were all carried out in a CH_3CN−THF (1:1) solution containing 2 M monomer, 1 mM CuBr/Me_6TREN, and 0.3 mM $CuBr_2$/2dnNbpy at 24 °C.

Scheme 2

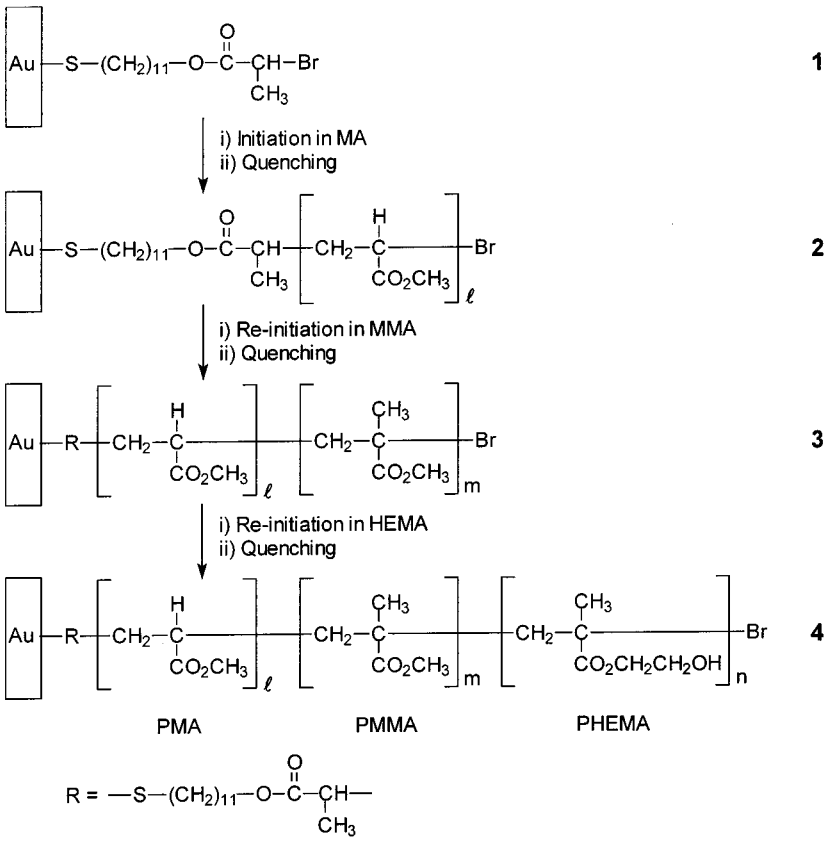

Quenching Procedure. To quench polymerization, we sequentially immersed substrates in three solutions of 0.02 M Cu(II)Br_2/2(dnNbpy) in 1:1 CH_3CN:THF. The substrates were then immersed in three vials containing the cosolvent and three vials of THF to remove Cu(II)Br_2 from the surface. After examination by reflectance FTIR spectroscopy, substrates were immersed in a solution containing another monomer/catalyst mixture to form the next block. When simple solvent rinsing was used rather than Cu(II)Br_2 quenching, the substrates were sequentially immersed in six separate CH_3CN:THF solutions.

Detachment of Polymer Brushes from Gold Surfaces. Polymer brushes were detached from gold surfaces by immersing the polymer-coated substrates in a 4 mM solution of I_2 in CH_2Cl_2 for 15 h at room temperature. After rinsing the surface with fresh CH_2Cl_2 and drying under a flow of N_2, the reflectance FTIR spectrum was measured to confirm that the polymer chains were detached from the surface. The initial CH_2Cl_2 solution was collected and transferred to a pear-shaped flask that was connected to a closed vacuum line. The solution was frozen in a liquid N_2 bath, and after opening the vacuum line, the bath was withdrawn, and the solvent was slowly removed under reduced pressure. After evaporation of CH_2Cl_2, a purplish thin coating remained on the inside of the flask. The flask was kept at 60 ± 10 °C in an oil bath, and I_2 was removed by sublimation under vacuum to yield a pale yellow coating on the flask. For GPC measurements, all of the remaining material in the flask was dissolved in ~150 μL of THF and injected into the instrument. Assuming full recovery of the polymer from a 380 Å thick PMMA film on ~8 cm^2 of gold surface, the concentration of detached polymer brushes in 150 μL of THF should have been ~0.2 mg/mL.

Analytical Methods. Reflectance FTIR spectroscopy was performed under nitrogen purging using a Nicolet Magna-IR 560 spectrometer (MCT detector) containing a PIKE grazing angle (80°) attachment. Ellipsometric measurements on polymer films were obtained with a rotating analyzer spectroscopic ellipsometer (model M-44; J.A. Woollam) at a 75° angle of incidence. Values of *n* and *k* were determined for bare gold at the 44 wavelengths (ranging from 414 to 751 nm) of the ellipsometer, and a wavelength-independent film refractive index of 1.5 was assumed when calculating film thicknesses from a fit to multiwavelength data. Gel permeation chromatography (GPC) was performed with two PLgel 10μ mixed-B columns and a PLgel 3μ mixed-E column in series and a Waters R410 differential refractometer detector (sensitivity set to 4). THF was used as the eluent at a flow rate of 1 mL/min at 35 °C, and monodisperse poly(methyl methacrylate) standards (Polysciences, Inc.) were used to calibrate the molecular weights. The molecular weights of PMMA standards were 350 000, 127 000, 30 000, and 6000 g/mol.

Results and Discussion

Synthesis of Tethered PMA-*b*-PMMA-*b*-PHEMA Brushes on Gold. To perform ATRP, a self-assembled monolayer of initiator, **1**, was immersed in a MA solution containing Cu(I)Br/Me_6TREN and Cu(II)Br_2/2(dnNbpy) at 25 °C. Although Cu(I)Br/Me_6TREN complexes are active and allow ATRP to proceed at room temperature, the presence of Cu(II)Br_2 is indispensable for controlling polymerization. Because of the poor solubility[18] of the Cu(II)Br_2 complex in neat monomer, we used a mixture of CH_3CN and THF (1:1 v:v) as a polar medium to obtain a homogeneous reaction system. These polar solvent mixtures should not restrict polymerization because ATRP is very tolerant toward functional groups such as ethers and nitriles.[16] After 20 min, the MA polymerization was quenched by transferring the substrate to a solution of Cu(II)Br_2/2(dnNbpy) in CH_3CN−THF (1:1). Matyjaszewski et al. reported that the Cu(II)Br_2 complex with dnNbpy acts as a deactivator and successfully controls surface-initiated ATRP, eliminating the need for sacrificial initiators.[12]

The formation of PMA on the surface is apparent from the appearance of a carbonyl peak at 1743 cm^{-1} in the

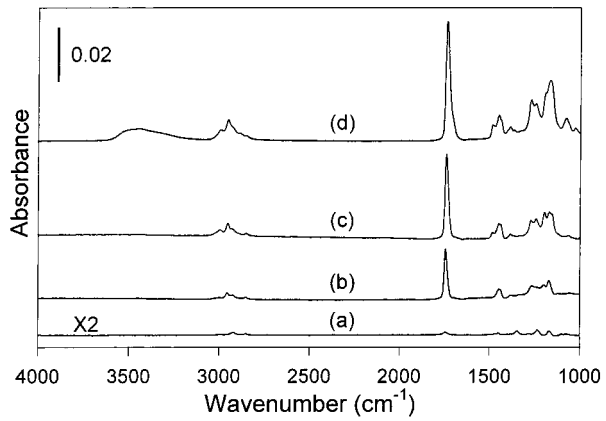

Figure 1. Reflectance FTIR spectra of (a) a layer of initiator immobilized on gold (**1**), (b) a grafted PMA layer on the initiator surface (**2**), (c) a grafted PMA-*b*-PMMA diblock copolymer (**3**), and (d) a grafted PMA-*b*-PMMA-*b*-PHEMA triblock copolymer (**4**).

reflectance FTIR spectrum of these films (Figure 1, spectrum b). After polymerization of the initial block, quenching, and washing with $CH_3CN-THF$, polymerization at **2** was reinitiated by transferring the substrate to a MMA solution containing fresh copper catalyst. Following the MMA polymerization, quenching, and washing, the reflectance FTIR spectrum of the film contained a more intense methyl peak at 2953 cm^{-1} and an increased carbonyl peak, confirming the formation of the PMMA block (Figure 1, spectrum c). Polymerization from **3** was then initiated in a HEMA solution at 40 °C. After the HEMA polymerization, the substrate was simply rinsed with a series of solvents including $CH_3CN-THF$, DMF, EtOAc, EtOH, and deionized water. Since little, if any, polymer formed in solution,[17] a simple solvent rinse was sufficient to clean the copolymer brushes on the surface. The appearance of a broad hydroxy (OH) peak at 3200−3600 cm^{-1} and a further increase in the intensity of the carbonyl peak (Figure 1, spectrum d) provide evidence for the formation of the third block, PHEMA. The ellipsometric thicknesses of the film after addition of each layer were as follows: **2**, 65 ± 1 Å; **3**, 133 ± 1 Å; and **4**, 271 ± 3 Å. The thicknesses were measured at three different spots on the same sample. Each succeeding polymer layer was purposely doubled in thickness by controlling polymerization time to provide clear changes in the IR spectrum after each polymerization cycle. Formation of the last block required longer polymerization times because fewer initiators were left on the surface (vide infra). Ellipsometry and FTIR spectroscopy showed that no polymerization occurred from a propionylated MUD SAM (no α-bromocarbonyl functionality) under the same polymerization and washing conditions used for the synthesis of each block of the triblock copolymer brushes. This result demonstrates that polymer grows only from surfaces with immobilized initiators.

Molecular Weights of Triblock Homopolymer Brushes. Comparison of the molecular weight distribution of block copolymer brushes with the corresponding distribution of brushes grown using a single initiation step should confirm block copolymer formation and demonstrate the efficiency of QR. If a significant fraction of initiating sites were lost during each QR step, the molecular weight distribution of the triblock brush would be broadened, resulting in a larger polydispersity index (PDI = M_w/M_n). To determine the molecular weights of polymer brushes, one must first detach the polymer chains from the substrate. We detached the brushes by exposure of the film to I_2, which is capable of breaking Au−S bonds.[19] After iodine treatment, detachment of PMMA chains was confirmed by reflectance FTIR and NMR. The FTIR spectrum of the I_2-treated surface did not show any significant residual polymer peaks, and the NMR spectrum of the collected polymer chains identified this material as PMMA.

Because of the insolubility of PHEMA,[20] we synthesized PMMA-*b*-PMMA-*b*-PMMA (triblock PMMA, which is in fact a homopolymer) by the QR strategy to confirm the formation of reasonably well-defined triblock chains. The average thickness of the three separate PMMA-*b*-PMMA-*b*-PMMA films we prepared was 381 ± 3 Å, including 16 Å for the initiator monolayer, and the thickness of each layer was about 120 Å. After detaching the PMMA brushes from the surface using iodine,[17,19] the molecular weight distribution was determined by GPC. The results shown in Table 1 (M_n = 37 400, PDI = 1.48) agree reasonably well with the values (M_n = 44 500, PDI = 1.30) for PMMA homopolymers grown by a single initiation step without QR.[17] This is strong evidence for formation of multiblock brushes, but the slightly lower M_n and higher PDI of PMMA-*b*-PMMA-*b*-PMMA may suggest a small amount of termination during QR cycles. However, the low signal-to-noise ratio in the chromatograms (Table 1) does not allow a firm conclusion to be drawn from these measurements. A second triblock polymer brush, PMA-*b*-PMA-*b*-PMA, synthesized by the QR strategy and characterized in the same way yielded M_n = 41 600 and PDI = 1.32 for 389 ± 2 Å thick films, showing that the quenching process is efficient.

Table 1 also includes two control experiments using commercial PMMA standards: runs a and b confirm that exposure of polymer chains to iodine should not affect M_n and PDI, while run c shows that the detection limit for PMMA in our GPC system (RI detector, THF as solvent) is <0.2 mg/mL. When the detached polymer brushes are dissolved in 150 μL of THF, their calculated concentration would be about 0.2 mg/mL, assuming that there is no loss during the workup procedure. The fact that the signal-to-noise ratio is a little higher for the control sample than for detached brushes indicates that some portion of the polymer brushes was probably lost during the microgram-scale workup and GPC sample injection. We also note that at these low polymer concentrations lower molecular weight species may be difficult to detect due to their minimal weight fraction. Additionally, the baseline at longer retention times is difficult to determine. Thus, the PDI values for the polymer brushes are probably artificially low.

Quantification of the Efficiency of QR. To quantify the efficiency of the QR process, we compared the thickness values of PMMA films prepared using several quenching ($Cu(II)Br_2$) and reinitiation cycles with values for films prepared with a single initiation step. The hollow circles in Figure 2 show the evolution of PMMA film thickness as a function of polymerization time when using a single initiation step. Films prepared with 1−3 QR cycles (triangles and diamond) have nearly the same thickness/time relationship, suggesting that almost 100% of the active polymerization sites were preserved during the quenching process.

Quantification of the quenching process requires a model of film growth because the rate of termination of

Table 1. GPC Data for PMMA Standards and Polymers Grown from a Surface using ATRP

polymer sample	GPC peak	measured M_n & PDI
PMMA standard sample, (a)–(c)		
(a) before iodine treatment	(a)	(a) M_n = 59,200 PDI = 1.07
(b) after iodine treatment	(b)	(b) M_n = 59,000 PDI = 1.07
(c) at low conc. 0.2 mg/mL	(c) 18.2 19.2 20.2 Minutes	(c) M_n = 62,700 PDI = 1.05
(d) Triblock PMMA (381 Å thick film)	(d) 16.6 19.4 22.2 Minutes	(d) M_n = 37,400 PDI = 1.48
(e) Triblock PMA (389 Å thick film)	(e) 17.6 19.8 22.0 Minutes	(e) M_n = 41,600 PDI = 1.32
(f) PMMA by single initiation step (370 Å thick film)	(f) 11.4 13.6 15.8 Minutes	(f) M_n = 44,500 PDI = 1.30

[a–c] The manufacturer-specified M_n and PDI values of the PMMA standard sample were 60 200 and 1.10, respectively. The standard was purchased from Polysciences, Inc. [b] The PMMA standard sample was dissolved in I_2/CH_2Cl_2 solution and kept at room temperature for 15 h. After removal of CH_2Cl_2 and I_2, the resulting PMMA was injected into the GPC instrument. [d,e] Triblock polymer brushes are, in fact, homopolymers synthesized by three cycles of quenching and reinitiation. For GPC analysis, these brushes were collected from three 2.7 cm^2 substrates (total area: ~8 cm^2). [c–e] The low signal-to-noise ratio is due to the low concentration of polymer. These peaks are magnified relative to a and b. [f] The elution time is faster than other runs because two PLgel 10μ mixed-B columns were used without an additional PLgel 3μ mixed-E column in series. The polymer brushes were collected from ~75 cm^2 surface area, yielding a relatively large amount of polymer chains and a higher signal-to-noise ratio than for the other polymer brushes.

growing chains is significant compared to the rate of polymerization from the surface. Loss of active chain ends during surface polymerization is implied by the nonlinear relationship between film thickness and time in Figure 2. This is consistent with solution ATRP using Me_6TREN, which also shows termination of growing chains.[18] A plot of thickness vs time for surface initiated ATRP of a sugar-carrying methacrylate using a CuBr/4,4′-di-*n*-heptyl-2,2′-bipyridine catalyst showed curvature[21] similar to that in Figure 2, while ATRP of methyl acrylate using CuBr/*N*,*N*,*N*′,*N*″,*N*″-pentamethyldiethylenetriamine (PMDETA) and $CuBr_2$/PMDETA showed a linear growth of polymer thickness with time.[12] The linear growth observed in the second example reflects a choice of monomer structure, catalytic system, and

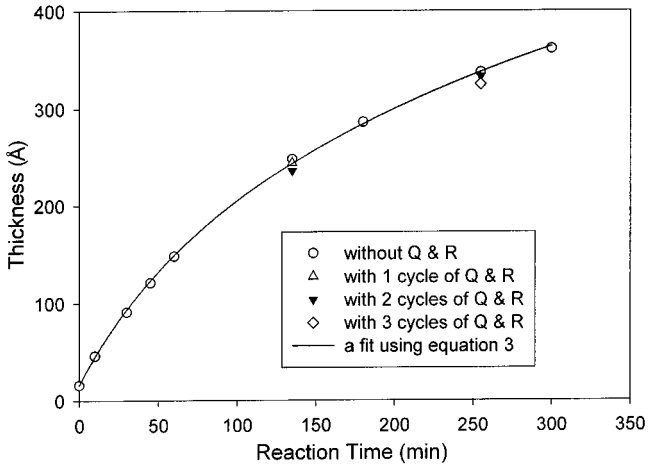

Figure 2. Ellipsometric thickness of PMMA films vs polymerization time. Thicknesses obtained at three different spots on a sample were averaged, and the standard deviation of these measurements was ±2 Å. For the case of Cu(II) quenching, polymerizations were quenched at 15 min or 15 min and 75 min. The line represents a fit to the thickness of films prepared in a single reaction step (open circles) using the function: thickness = $16 + A \ln(1 + Bt)$.

reaction medium that minimizes termination by recombination reactions. ATRP of ethylene glycol dimethacrylate in aqueous media also showed a reasonably linear growth of polymer thickness with time.[22]

To account for the loss of growing chains during polymerization from a surface, we utilize a simple kinetic model for film growth. We assume that the loss of active chains, *A*, is second order with respect to surface concentration as represented by eq 1 Note that

$$\frac{d[A]}{dt} = -k_1[A]^2 \tag{1}$$

A includes chain ends in both the dormant and radical states. The increase in film thickness with time, d*l*/d*t*, should be first order with respect to the number of active chains as shown in eq 2. Integration of eq 1 yields an

$$\frac{dl}{dt} = k_2[A] \tag{2}$$

expression for the surface concentration of active chains at any given time, and insertion of this expression into eq 2 followed by integration yields an expression for film thickness as a function of time (eq 3), where $[A^0]$ is the

$$l = \frac{k_2}{k_1} \ln(1 + k_1[A^0]t) \tag{3}$$

initial concentration of active initiator functionalities. The fit of the data in Figure 2 (open circles) to this equation is excellent, showing that the model is reasonable. (The fit to the data also includes addition of the thickness of the initiator monolayer to eq 3.)

To account for the loss of chain ends during quenching and reinitiation, we introduce a quenching efficiency, *Q*, that is the ratio of active chains after and before quenching. Thus, if the first quenching step occurs at time t_1, the number of active sites after the quenching step will be given by eq 4. For multiple quenching steps, the concentration of active sites after quenching step *n* (which occurs at time t_n) is given by eq 5, where *n* is

the number of quenching steps and the t_n values represent the times at which each of the quenching steps occurred. The growth in film thickness, Δl between the $(n-1)$th and nth quenching steps will thus be given by eq 6. This equation is obtained by substituting values of $[A(t_{n-1})]$ for $[A^0]$ and values of $(t_n - t_{n-1})$ for t in eq 3. The total film thickness is simply the sum of the Δl_n values.

$$[A] = \frac{[A^0]Q}{1 + k_1[A^0]t_1} \quad (4)$$

$$[A(t_n)] = [A^0]Q^n/\{1 + k_1[A^0]t_1 + Qk_1[A^0](t_2 - t_1) + Q^2k_1[A^0](t_3 - t_2) + ... + Q^{n-1}k_1[A^0](t_n - t_{n-1}))\} \quad (5)$$

$$\Delta l_n = \frac{k_2}{k_1}\ln(1 + k_1[A^0]Q^{n-1}(t_n - t_{n-1})/\{1 + k_1[A^0]t_1 + Qk_1[A^0](t_2 - t_1) + Q^2k_1[A^0](t_3 - t_2) + ... + Q^{n-2}k_1[A^0](t_{n-1} - t_{n-2})\} \quad (6)$$

Using eq 6 and the data in Figure 2, we estimated the efficiency of quenching, Q. These calculations show that $Q > 0.95$ as would be expected from the similar thicknesses of films prepared in a single step and films prepared with quenching and reinitiation. The effect of quenching will be more pronounced as termination of active chains is reduced or as the number of quenching steps increases. In the next section we compare thicknesses of films prepared using up to six quenching steps and two different quenching procedures.

Comparison of Cu(II)Br$_2$ Quenching with Simple Solvent Washing. Considering the short lifetime of radicals in ATRP,[23] their concentration at any given time should be very low. The combination of this low radical concentration and the inertness of the dormant chain ends might allow replacement of the Cu(II)Br$_2$ quenching with simple solvent washing to remove unreacted monomer after each block is formed. Matyjaszewski[24] and Dadmun[25] reported recently that multiblock copolymers could be prepared by ATRP in solution without a quenching step. However, in some cases, polydispersity slightly increased with the number of blocks, implying that some termination of polymer chains happens during separation and reinitiation procedures.[25] This trend led us to use the Cu(II) quenching strategy to shift the equilibrium to inert dormant chains during separation and reinitiation procedures. Cu(II) quenching might be especially important for the preparation of copolymer brushes because chain ends growing from surfaces are in close proximity and may recombine more readily than similar chains in solution.

To see whether the Cu(II) quenching step is necessary, we quenched polymerizations either with a Cu(II)Br$_2$ solution or with solvent washing after formation of each block. FTIR spectroscopy and ellipsometry show that both approaches led to the successful formation of multiblock polymer brushes. However, films prepared using the solvent washing protocol repeatedly showed subsequent block thicknesses that were 2−4% lower than those achieved by the QR strategy. To determine whether this difference was significant, we prepared a heptablock PMMA film ([PMMA-*b*-]$_6$PMMA) with and without Cu(II)Br$_2$ quenching steps. We either quenched

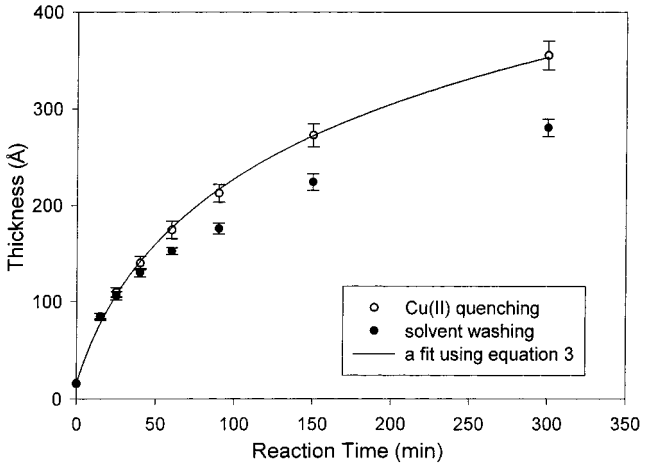

Figure 3. Thickness of multiblock PMMA films vs polymerization time. Each subsequent point represents one more cycle of polymerization followed by Cu(II) quenching or solvent washing; e.g., 300 min data were obtained after seven polymerization steps with quenching or washing between each step. Error bars represent the standard deviations of thickness determinations on at least three different spots on two different samples. The line represents a fit to the thickness of films prepared with Cu(II)Br$_2$ quenching (open circles) using the function: thickness $= 16 + A\ln(1 + Bt)$.

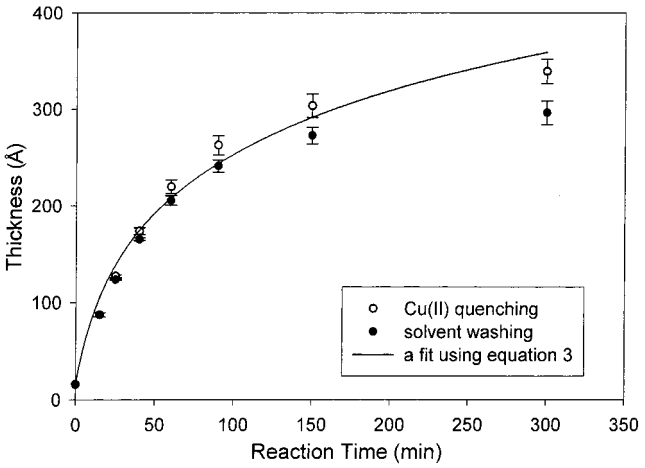

Figure 4. Thickness of multiblock PMA films vs polymerization time. Each subsequent point represents one more cycle of polymerization followed by Cu(II) quenching or solvent washing. Error bars represent the standard deviations of thickness determinations on at least three different spots on two different samples. The line represents a fit to the thickness of films prepared with Cu(II)Br$_2$ quenching (open circles) using the function: thickness $= 16 + A\ln(1 + Bt)$.

or solvent-washed polymer films after 15, 25, 40, 60, 90, and 150 min of reaction time and reinitiated to prepare the next block. Figure 3 shows that as the number of QR cycles increased, the difference in the thicknesses of films synthesized by the two methods also increased. We also prepared heptablock PMA films ([PMA-*b*-]$_6$PMA) using both Cu(II)Br$_2$ quenching and solvent washing, and the results are shown in Figure 4. Again, the higher efficiency of the Cu(II)Br$_2$ quenching strategy becomes evident as the number of quenching steps increases. After heptablock formation, the accumulated difference in the thicknesses of the samples prepared by the two methods were 21% and 13% for [PMMA-*b*-]$_6$PMMA and [PMA-*b*-]$_6$PMA, respectively. Presumably, the termination of some active chains during solvent washing results in fewer growing chains and lower thicknesses.

Assuming that the Cu(II)Br_2 quenching step had an efficiency of 100%, we fit the data for PMMA film growth (open circles, Figure 3) using eq 3. This allowed us to obtain values for k_2/k_1 and $k_1[A^0]$. Using these values and eq 6, we estimated Q for solvent washing and found it to be around 87%. Thus, the Cu(II) quenching method is considerably more efficient than solvent washing. In the case of PMA, the fit of the thickness data for Cu(II) quenching to eq 3 was not sufficiently good to estimate the quenching efficiency for the solvent washing procedure. However, the data clearly show the lower efficiency of solvent washing compared to Cu(II) quenching. The low quenching efficiency for solvent washing is somewhat surprising as ATRP usually results in a low concentration of radicals.

Conclusion

Surface-initiated ATRP was successfully quenched by a Cu(II)Br_2/2(dnNbpy) solution, and dormant initiating sites were preserved for reinitiation of multiblock synthesis. Direct GPC measurement of the molecular weights of polymer brushes detached from the surface demonstrates that this QR method is capable of producing relatively homogeneous brushes. Reflectance FTIR spectroscopy, ellipsometry, and molecular weight data confirm the formation of triblock copolymer brushes on gold surfaces. The efficiency of a Cu(II)Br_2 QR cycle determined from the growth rate of PMMA films was >95%, while the same efficiency for solvent washing was 85−90%. The Cu(II)Br_2 QR approach allows preparation of multiblock copolymers with control over the thickness of each block at ambient temperature.

Acknowledgment. We thank the NSF Center for Sensor Materials at Michigan State University for financial support of this research.

References and Notes

(1) (a) Dan, N.; Tirrell, M. *Macromolecules* **1993**, *26*, 4310−4315. (b) Hadziioannou, G.; Patel, S.; Granick, S.; Tirrell, M. *J. Am. Chem. Soc.* **1986**, *108*, 2869−2876.
(2) Morkved, T. L.; Lu, M.; Urbas, A. M.; Ehrichs, E. E.; Jaeger, H. M.; Mansky, P.; Russell, T. P. *Science* **1996**, *273*, 931−933.
(3) Thurn-Albrecht, T.; Schotter, J.; Kastle, G. A.; Emley, N.; Shibauchi, T.; Krusin-Elbaum, L.; Guarini, K.; Black, C. T.; Tuominen, M. T.; Russell, T. P. *Science* **2000**, *290*, 2126−2129.
(4) Kim, H.-C.; Jia, X.; Stafford, C. M.; Kim, D. H.; McCarthy, T. J.; Tuominen, M.; Hawker, C. J.; Russell, T. P. *Adv. Mater.* **2001**, *13*, 795−797.
(5) Mansky, P.; Liu, Y.; Huang, E.; Russell, T. P.; Hawker, C. J. *Science* **1997**, *275*, 1458−1460.
(6) Zhao, B.; Brittain, W. J. *Prog. Polym. Sci.* **2000**, *25*, 677−710.
(7) Zhao, B.; Brittain, W. J. *J. Am. Chem. Soc.* **1999**, *121*, 3557−3558.
(8) Sedjo, R. A.; Mirous, B. K.; Brittain, W. J. *Macromolecules* **2000**, *33*, 1492−1493.
(9) Zhao, B.; Brittain, W. J.; Zhou, W.; Cheng, S. J. D. *Macromolecules* **2000**, *33*, 8821−8827.
(10) (a) Corkery, R. W. *Langmuir* **1997**, *13*, 3591−3594. (b) Alberti, G.; Casciola, M.; Costantino, U.; Vivani, R. *Adv. Mater.* **1996**, *8*, 291−303. (c) Katz, H. E. *Chem. Mater.* **1994**, *6*, 2227−2232. (d) Kaschak, D. M.; Mallouk, T. E. *J. Am. Chem. Soc.* **1996**, *118*, 4222−4223. (e) Decher, G. *Science* **1997**, *277*, 1232−1237.
(11) (a) Zhao, B.; Brittain, W. J. *Macromolecules* **2000**, *33*, 8813−8820. (b) Huang, X.; Wirth, M. J. *Macromolecules* **1999**, *32*, 1694−1696.
(12) Matyjaszewski, K.; Miller, P. J.; Shukla, N.; Immaraporn, B.; Gelman, A.; Luokala, B. B.; Siclovan, T. M.; Kickelbick, G.; Vallant, T.; Hoffmann, H.; Pakula, T. *Macromolecules* **1999**, *32*, 8716−8724.
(13) Husseman, M.; Malmstrom, E. E.; McNamara, M.; Mate, M.; Mecerreyes, D.; Benoit, D. G.; Hedrick, J. L.; Mansky, P.; Huang, E.; Russell, T. P.; Hawker, C. J. *Macromolecules* **1999**, *32*, 1424−1431.
(14) Davis, K. A.; Paik, H.-j.; Matyjaszewski, K. *Macromolecules* **1999**, *32*, 1767−1776.
(15) Ciampolini, M.; Nardi, N. *Inorg. Chem.* **1966**, *5*, 41−44.
(16) Matyjaszewski, K.; Patten, T. E.; Xia, J. *J. Am. Chem. Soc.* **1997**, *119*, 674−680.
(17) Kim, J.-B.; Bruening, M. L.; Baker, G. L. *J. Am. Chem. Soc.* **2000**, *122*, 7616−7617.
(18) Queffelec, J.; Gaynor, S. G.; Matyjaszewski, K. *Macromolecules* **2000**, *33*, 8629−8639.
(19) Templeton, A. C.; Hostetler, M. J.; Kraft, C. T.; Murray, R. W. *J. Am. Chem. Soc.* **1998**, *120*, 1906−1911.
(20) (a) Robinson, K. L.; Khan, M. A.; de Paz Báñez, M. V.; Wang, X. S.; Armes, S. P. *Macromolecules* **2001**, *34*, 3155−3158. (b) Huang, W.; Kim, J.-B.; Baker, G. L.; Bruening, M. L. *Macromolecules* **2002**, *35*, 1175−1179.
(21) Ejaz, M.; Ohno, K.; Tsujii, Y.; Fukuda, T. *Macromolecules* **2000**, *33*, 2870−2874.
(22) Huang, W.; Baker, G. L.; Bruening, M. L. *Angew. Chem., Int. Ed.* **2001**, *40*, 1510−1512.
(23) Matyjaszewski. K. *Macromolecules* **1999**, *32*, 9051−9053.
(24) Davis, K. A.; Matyjaszewski, K. *Macromolecules* **2001**, *34*, 2101−2107.
(25) Eastwood, E. A.; Dadmun, M. D. *Macromolecules* **2001**, *34*, 740−747.

MA011736Z